RSC Advances

PAPER

View Article Online
View Journal | View Issue



Cite this: *RSC Adv.*, 2014, **4**, 62895

# Calixarene modified montmorillonite: a novel design for biosensing applications†

Burak Sonmez,[a] Serkan Sayin,[b] Esra Evrim Yalcinkaya,[c] Didem Ag Seleci,[a] Huseyin Bekir Yildiz,[b] Dilek Odaci Demirkol*[ad] and Suna Timur*[ad]

Received 5th October 2014
Accepted 6th November 2014

DOI: 10.1039/c4ra11818a

www.rsc.org/advances

Here we report the synthesis, characterization and application of calixarene (Calix) modified montmorillonite (Mt) as a platform for bio-applications such as biomolecule immobilization and biosensing technologies. This modification enhanced the biomolecule immobilization capability of Mt. Initially, amino-functionalised calixarenes (Calix-$NH_2$) were synthesized and used as a modifier. X-ray diffraction, Fourier transform infrared spectroscopy, zeta potential and thermal gravimetric analysis were performed to verify the modification of the clay minerals. For the biosensor construction, Calix-$NH_2$ modified Mt (Calix-$NH_2$/Mt), bovine serum albumin (BSA), glutaraldehyde (GA) and pyranose oxidase were immobilized on the surface of a glassy carbon electrode which was then referred to as a Calix-$NH_2$/Mt/PyOx biosensor. After optimization of the enzyme amount and pH, analytical characteristics were investigated in detail.

## Introduction

Immobilization of the enzymes in a suitable matrix is crucial for fabrication of biosensor systems and other enzyme-based diagnostic techniques. In the literature, various techniques and immobilization materials have been attempted to fabricate enzyme biosensors.[1–5] Clays are one of the advantageous materials to design different immobilization matrices for biomolecule immobilization due to their high stability, good adsorptive capacity, large specific surface area, stick out adhesiveness and low costs.[6] Laponite, montmorillonite (Mt), nontronite and layered doublehydroxides (LDHs) are well known smectite clay minerals that already were exploited in numerous biosensor studies.[7–11] Mt is a naturally occurring cationic phyllosilicate and composed of silica tetrahedral sheets layered between alumina octahedral sheets. To date it has been utilized in different biotechnological and biomedical applications.[12–14] For instance, Joshi *et al.* used Mt as drug carrier for timolol maleate and demonstrated the intercalation of timolol maleate into the interlayer of Mt at different pH.[15] Folic acid modified Mt was used as a cell specific adhesion material for HeLa cells.[16] Demir *et al.* were successfully applied trimethylamine modified Mt to design microbial biosensor systems.[17] Besides, glucose oxidase and laccase were also, immobilized on dimethylamine and histidine modified Mt matrices for glucose and phenol sensing, respectively.[9,18]

Calixarenes which are cyclic oligomers, are synthesized traditionally *via* oligomerization of phenol and formaldehyde.[19] Due to their excellent ability to form host–guest complexes and their multi center bonding with guest molecules, calixarenes can selectively bind different inorganic and organic compounds.[20–22] Chen *et al.* reported the synthesis of *p-tert*-butylthiacalix[4]arene tetra-amine and demonstrated the use of calixarenes as enzyme immobilization material.[23] Recently, 5,11,17,23-tetra-*tert*-butyl-25,27-bis(3-thiol-1-oxypropane)-26,28-dihydroxycalix[4]arene (SH-Calix) was synthesized and used to modify gold electrode *via* formation of self-assembled monolayers. Then, glucose oxidase was immobilized on the SH-Calix-modified surface.[24]

This work composed of three parts as follows; (i) the synthesis and characterization of 5,17-diamino-25,27-bis[*N*-(2-aminoethyl)]calix[4]azacrown(Calix-$NH_2$), (ii) modification of Mt with Calix-$NH_2$ salt which is then, used as a platform for the enzyme immobilization, (iii) biosensor (Calix-$NH_2$/Mt/PyOx) applications. Pyranose oxidase (PyOx) was selected as a model enzyme. Glutaraldehyde (GA) and bovine serum albumin (BSA) were used to test the specificity of the sensor. Amine groups of Calix-$NH_2$ played an important role in the stabile immobilization of the enzyme by crosslinking with GA. Calix-$NH_2$, BSA, GA and PyOx were mixed and immobilized onto glassy carbon electrode (GCE). The enzymatic reaction of PyOx is given below;[25]

[a]*Ege University Faculty of Science, Biochemistry Department, 35100 Bornova-Izmir, Turkey. E-mail: suna.timur@ege.edu.tr; dilek.odaci.demirkol@ege.edu.tr*

[b]*KTO Karatay University, Department of Materials Science and Nanotechnology Engineering, 42020 Konya, Turkey*

[c]*Ege University Faculty of Science, Chemistry Department, 35100 Bornova-Izmir, Turkey*

[d]*Ege University, Institute of Drug Abuse Toxicology &Pharmaceutical Sciences, 35100 Bornova-Izmir, Turkey*

† Electronic supplementary information (ESI) available. See DOI: 10.1039/c4ra11818a

$$\text{D-Glucose} + O_2 \rightleftharpoons \text{2-dehydro-D-glucose} + H_2O_2$$

The consumption of the oxygen due to the enzymatic activity was related to the substrate concentration. The response signals were followed at −0.7 V *vs.* Ag/AgCl. After optimization studies, Calix-$NH_2$/Mt/PyOx biosensor was calibrated for glucose and applied for the glucose analysis in a real sample.

# Materials and methods

## Materials

Pyranose oxidase (EC 1.1.3.10, from *Coriolus* sp., ≥ 2.7 units per mg), GA solution (25%, v/v), bovine serum albumin (BSA) glucose and all other chemicals were ordered from Sigma Aldrich. Mt was supplied by Southern Clay Products, Inc. (CEC = 92 meq per 100 g). Thin layer chromatography (TLC) analyses were carried out on DC Alufolien Kieselgel 60 $F_{254}$ (Merck). The solvents were dried by storing them over molecular sieves (Aldrich; 4 Å, 8–12 mesh). All reactions, unless otherwise noted, were conducted under nitrogen atmosphere. All starting materials and reagents used were of standard analytical grade from Merck or Aldrich and used without further purification. All aqueous solutions were prepared with deionized water that was passed through a Millipore Milli-Q Plus water purification system.

## Synthesis of Calix-$NH_2$

*p-tert*-Butylcalix[4]arene (**1**), calix[4]arene (**2**), 1,3-*O*-dimethyl ester calix[4]arene derivative **3** and the compound **4** *N*-(2-aminoethyl)calix[4]azacrown were synthesized according to literature procedures.[26–29] The compounds **5** 5,17-dinitro-25,27-bis[*N*-(2aminoethyl)]calix[4]azacrown and **6** 5,17-diamino-25,27-bis[*N*-(2-aminoethyl)]calix[4]azacrown are herein reported for the first time.

## Synthesis of compound 4

Yield; 70.5%, m.p.; 250–252 °C.FTIR (ATR): 1678 $cm^{-1}$ (C=O). $^1$H NMR (400 MHz $CDCl_3$): $\delta$ 2.13–2.33 (m, 2H, –$NH_2$), 2.53 (t, 2H, $J$ = 5.6 Hz, –$CH_2$–N), 2.74–2.81 (m, 6H, –$CH_2$–), 3.46 (d, 4H, $J$ = 13.6 Hz, Ar–$CH_2$–Ar), 3.53–3.56 (m, 4H, –$CH_2$–), 4.21 (d, 4H, $J$ = 13.6 Hz, Ar–$CH_2$–Ar), 4.55 (s, 4H, O–$CH_2$–), 6.73–6.79 (m, 4H, ArH), 6.85 (d, 4H, $J$ = 7.6 Hz, ArH), 7.12 (d, 4H, $J$ = 7.6 Hz, ArH), 7.19 (s, 2H, –OH), 8.32 (t, 2H, $J$ = 5.6 Hz, –NH). Anal. Calcd. for $C_{38}H_{42}N_4O_6$: C, 70.13; H, 6.51; N, 8.61. Found (%); C, 70.05; H, 6.63; N, 8.55.

## Synthesis of compound 5

$HNO_3$ (65%, 20 mL) was added to the solution of **4** (0.7 g, 1.076 mmol) in 20 mL of $CH_2Cl_2$. The mixture was stirred at room temperature for 1 h. Then, 50 mL water was poured into the mixture, and then, filtered. The solid was washed with water to neutralize and then, dried. The crude was recrystallized from acetone. Yield; 56.5%, m.p.; 208–210 °C.FTIR (ATR): 1660 $cm^{-1}$(C=O). $^1$H NMR (400 MHz DMSO): $\delta$ 2.60–2.70 (m, 5H, –$CH_2$– and –$^+NH_3$), 3.15–3.47 (m, 6H, –$CH_2$–over shielded by the solvent), 3.69–3.73 (m, 8H, –$CH_2$– and Ar–$CH_2$–Ar), 4.19–4.30 (m, 4H, Ar–$CH_2$–Ar), 4.58 (brs, 4H, O–$CH_2$–), 6.89 (t, 2H, $J$ = 7.6 Hz, ArH), 7.21 (d, 4H, $J$ = 7.6 Hz, ArH), 7.63 (brs, 2H, –OH), 8.18–8.24 (m, 6H, ArH and –NH). Anal. Calcd. For $C_{38}H_{41}N_6O_{10}$: C, 61.53; H, 5.57; N, 11.33. Found (%); C, 61.44; H, 5.81; N, 11.38.

## Synthesis of compound 6

Raney Ni (1.0 g) was added to the solution of **5** (0.35 g, 0.473 mmol) and hydrazine monohydrate (2.8 mL) in MeOH. The reaction mixture was refluxed for 10 h. The reaction temperature was then cooled to room temperature, and then, filtered and evaporated to dryness. The crude was recrystallized from acetone. Yield: %95, m.p.; 269–272 °C. FTIR (ATR): 1660 $cm^{-1}$(C=O). $^1$H NMR (400 MHz DMSO): $\delta$ 2.69 (t, 3H, $J$ = 4.4 Hz, –$^+NH_3$), 2.92–2.95 (m, 2H, –$CH_2$–), 3.16–3.45 (m, 10H, –$CH_2$– over shielded by the solvent), 3.63–3.74 (m, 4H, Ar–$CH_2$–Ar), 3.98–4.04 (m, 8H, Ar–$CH_2$–Ar and Ar–$NH_2$), 4.52–4.59 (m, 4H, O–$CH_2$–), 6.89 (t, 2H, $J$ = 7.6 Hz, ArH), 7.21 (d, 4H, $J$ = 7.6 Hz, ArH), 7.57–7.74 (m, 2H, –OH), 7.99–8.23 (m, 6H, ArH and –NH). $^{13}$C NMR (100 MHz DMSO): $\delta$ 31.07 (Ar–*C*$H_2$–Ar), 37.26 (NH–*C*$H_2$), 38.98 ($NH_2$–*C*$H_2$), 53.04 (N–*C*$H_2$), 54.81 (N–*C*$H_2$), 74.20 (O–*C*$H_2$), 124.96 (Ar–*C*), 126.02 (Ar–*C*), 129.46 (Ar–*C*), 130.10 (Ar–*C*), 133.56 (Ar–*C*), 144.60 ($NH_2$–Ar–*C*), 152.99 (ArO–*C*), 153.60 (ArO–*C*), 169.26 (*C*=O). Anal. Calcd. For $C_{38}H_{45}N_6O_6$: C, 66.94; H, 6.65; N, 12.33. Found (%); C, 67.01; H, 6.73; N, 12.28.

## Preparation of Calix-$NH_2$/Mt

The Mt was organically modified by a cation-exchange reaction between Mt and Calix-$NH_2$. The Calix-$NH_2$, as an intercalating agent, was firstly protonated with 1.0 M HCl aqueous solutions to adjust the pH to 2.0–3.0. The required amount (two time equivalent of the CEC) of the Calix-$NH_2$ salt was dissolved in deionized water at approximately 50 °C. 1.0 g of Mt was preliminarily dispersed in deionized water by using a mechanical stirrer. The Calix-$NH_2$ solution was added to the dispersion of the clay mineral particles, and the mixture was exchanged for 24 h at room temperature using vigorous stirring. The resulted organo-clay mineral (Calix-$NH_2$/Mt) was collected by filtration and repeatedly washed with hot deionized water until no chloride ions were detected upon adding 0.1 M aqueous $AgNO_3$. It was dried in a vacuum oven at 50 °C for 2 days to a constant weight.

## Characterization of Calix-$NH_2$/Mt

For the characterization, initially, modified and pristine samples were examined by X-ray diffraction (XRD) Spectrometers (Philips E'xpert Pro; Cu-K$\alpha$ radiation, $\lambda$ = 1.54056 Å) to determine the interlayer spaces of Mt and Calix-$NH_2$/Mt. The samples were scanned under the diffraction angle 2$\theta$in the range of 4.0–70.0 with a scanning rate of 2.0 $min^{-1}$. The interlayer distance was determined by the diffraction peak, using the Bragg equation ($n\lambda = 2d \sin\theta$). Fourier transform infrared (FTIR) spectra of clay minerals were recorded using a Perkin Elmer Pyris 1 FTIR Spectrometer with KBr pellet. Thermal degradation was studied with a thermogravimetric analyzer (Perkin Elmer Pyris 1 TGA/DTA) by heating the samples from

 

ambient temperature to 1000 °C at 10 °C $min^{-1}$ under a 10 bar dry air atmosphere. The electrokinetic properties of clay minerals were determined by measuring the zeta-potential of particles with a Zeta-Meter 3.0+ (with a Zeiss DR microscope, GT-2 type quartz cell, molybdenum-cylinder anode, and platinum-rod cathode electrode). For this purpose, the clay mineral samples were stirred overnight in the deionized water to obtain well dispersed particles. The zeta potential of the Mt dispersions was estimated from the measured electrophoretic mobility by employing the Smoluchowski equation.[30] The value of the zeta potential assigned to the dispersions was the average of the data obtained from at least 10 experiments. All of the samples were dried in a vacuum oven before the analyses at 50 °C for 2 days.

Scanning Electron Microscopy (SEM) images were registered by using SEM (JEOL5600-LU). The images were taken *via* using an acceleration voltage of 20 kV.

### Calix-$NH_2$/Mt biosensor

Glassy carbon electrodes (GCE) were polished with 0.5 mm alumina slurry. To remove alumina residues on the electrode, ultrasonic cleaning for about 2–3 min in 1 : 1 ethanol distilled water was carried out. Afterwards, 1.0 mg PyOx (in 2.5 μL, sodium phosphate buffer pH 7.0, which equals to 2.7 units), 5.0 μL of Calix-$NH_2$/Mt solution (1.0 mg $mL^{-1}$ in sodium phosphate buffer pH 7.0), 2.5 μL of BSA (1.0 mg $mL^{-1}$ in sodium phosphate buffer, pH: 7.0) and 2.5 μL of glutaraldehyde (5.0%, in sodium phosphate buffer, pH 7.0) were mixed. Finally, 12.5 μL of this mixture was dropped on the electrode surface and allowed to dry at room temperature for 1 h. The same procedure was used to prepare the Mt modified PyOx biosensors in which only pristine Mt was used instead of Calix-$NH_2$ modified clay mineral.

### Electrochemical measurements

Amperometric measurements performed using a Palm Sens Potentiostat (Palm Instruments, Houten, Netherlands). All experiments were carried out in a reaction cell in working buffer (10 mL sodium phosphate buffer, 50 mM, pH 6.0) at room temperature using of three electrode configuration. GCE as a working electrode, Ag/AgCl as a reference electrode (3.0 M KCl, Metrohm, Switzerland) and Pt as a counter electrode (Metrohm, Switzerland) were used. Initially, the biosensors were equilibrated in the working buffer in the reaction cell and then, glucose was added. The response signals which were proportional to the substrate concentration were followed at −0.7 V *vs.* Ag/AgCl. The consumption of molecular oxygen in the enzymatic reaction was monitored at given potential. PyOx oxidizes glucose to 2-dehydro-D-glucose and the signals were correlated indirectly to the substrate concentrations consumed during the enzymatic reaction.[9,17,18,24]

After each measurement, the electrodes were washed with distilled water and the working buffer was refreshed.

### Sample application

Calix-$NH_2$/Mt/PyOx biosensor was used to analyze the glucose concentration in coke and fizzy samples. The sample was also analyzed with Trinder reagent which is a commercial enzyme assay kit based on spectrophotometric analysis. This assay includes oxidation of glucose to D-gluconate catalyzed by glucose oxidase with the formation of hydrogen peroxide. In the presence of peroxidase, a mixture of phenol and 4-aminoantipyrine is oxidized by hydrogen peroxide to form a red quinineimine dye proportional to the glucose concentration in the sample.[31] The glucose concentration in the real sample was measured by direct addition of samples into working buffer, instead of glucose. The amount of glucose in the samples was calculated from corresponding calibration curves obtained with the standard glucose solutions.

## Results

### Synthesis of a calixarene derivative substituted at the both rims with primary amine groups

*p-tert*-Butylcalix[4]arene**1** was chosen as the starting material, and it was transformed to the dealkylated derivative **2** and then the diester derivative **3** according to known procedures (see Scheme 1).[26–28] Treatment of the diester derivative **3** with tris(2-aminoethyl\mine in the presence of MeOH/toluene led to produce compound **4** according to the literature procedure.[29] Then, a mixture of compound **4** with 65% $HNO_3$ in DCM was reacted at room temperature for 1 h yielded the *p*-nitro substituted derivative **5**. Upon reduction of nitro groups with Raney-Ni, the target compound **6**, which was functionalized at

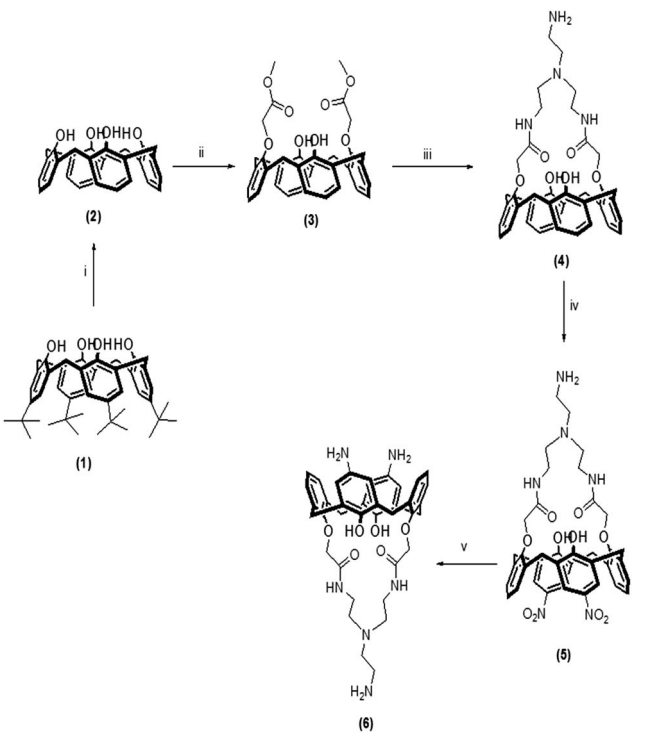


Scheme 1 The synthetic route for compound 6. Reaction conditions: (i) Phenol, $AlCl_3$; (ii) $K_2CO_3$, $CH_3CN$, methylbromoacetate; (iii) Tris (2-aminoethyl)amine, MeOH/toluene; (iv) $HNO_3$, $CH_2Cl_2$; (v) Raney-Ni, hydrazine, MeOH.

the both rims of Calix with the primary amine groups, was synthesized in 95% yield (see Scheme 1).

The characterization of the synthesized Calix derivatives was performed by FTIR, $^1$H and $^{13}$C NMR spectroscopy and given as ESI (Fig. S1–S5†). The FTIR spectra of **4–6** signify that their characteristic peaks(C═O) appear at 1678 cm$^{-1}$ for **4** and 1660 cm$^{-1}$ for both **5** and **6** (Fig. S1†). In the$^1$H NMR spectrum of **4**, the additional peaks of Tris (2-aminoethyl) aiming at $\delta$ 2.13–2.33 (m, 2H, –N**H**$_2$), 2.53 (t, 2H, $J$ = 5.6 Hz, –C**H**$_2$–N), 2.74–2.81 (m, 6H, –C**H**$_2$–), 3.53–3.56 (m, 4H, –C**H**$_2$–) and 8.32 ppm (t, 2H, $J$ = 5.6 Hz, –N**H**) placed on the spectrum. Thus, these peaks confirm the structure of **4** (Fig. S2†).[1] H NMR spectrums of **5** which are nitro derivative of **4** clearly verifies the structure of **5** by disappearing of two protons of aromatic at *para* positions on the spectrum (Fig. S3†). Obtained compound **6** by reduction of nitro groups has four protons at 3.98 ppm belonging Ar–NH$_2$ groups in the $^1$H-NMR spectrum (Fig. S4†). In addition, in the $^{13}$C NMR spectra of **6**, it can be seen the peak belonging to the *C*═O groups appears at 169.26 ppm, (Fig. S5†).

### Characterization of Calix-NH$_2$/Mt

Each layer of natural Mt consists of octahedrally coordinated cations (typically Mg, Al and Fe) sandwiched by tetrahedrally coordinated cations (typically Si and Al). Isomorphous substitution of $Si^{4+}$ by $Al^{3+}$ leads to a net negative surface charge that is compensated by an interlayer of exchangeable, hydrated cations ($Ca^{2+}$, $Mg^{2+}$, $Cu^{2+}$, $Na^{+}$, $H^{+}$). The surface of Mt is hydrophilic and this makes difficult the interaction of the clay mineral with the enzyme substrate. Therefore, it is necessary to make the surface of Mt less hydrophilic to compatible with a chosen enzyme. Various methods have been proposed for making clay minerals more hydrophobic.[32] In our case, the methodology is based on the replacement of the exchangeable hydrated cations with organophilic cations. The clay minerals were characterized by FTIR, XRD, TGA/DTG and zeta potential measurements. The FTIR spectra of pristine Mt and Calix-NH$_2$/Mt are presented in Fig. 1. In the FTIR spectrum of Mt (Fig. 1A), the band at 3630 cm$^{-1}$ is ascribed the –OH bond corresponding to the characteristic stretching for Al–Al–OH bond in the octahedral layer of Mt. The band at around 1630 cm$^{-1}$ is related with H–OH stretching vibration. An intense peak at around 1000 cm$^{-1}$ is the characteristic absorption band for Mt corresponding to Si–O stretching. After modification with Calix-NH$_2$ (Fig. 1B) characteristic absorption bands for both Mt and modifier were observed. In addition to Mt band, characteristic peaks (C═O) of Calix-NH$_2$ were shifted towards to 1730 cm$^{-1}$. Also, vibration peaks at 2980 cm$^{-1}$ and 2850 cm$^{-1}$ for –CH stretching and at 1360 cm$^{-1}$ for –CH$_2$ bending are observed, supporting the intercalation of Calix-NH$_2$ salt between the silicate layers.

The X-ray diffraction (XRD) technique is frequently used to detect the basal spacing between the interlayer of the clay mineral particles. XRD pattern of pristine Mt and Calix-NH$_2$/Mt is shown in Fig. 2 Pristine Mt yields characteristic diffraction peaks at $2\theta$ = 7.74. This diffraction peak corresponds to the basal spacing $d_{001}$(11.4 Å). From the XRD pattern of Calix-NH$_2$/Mt (Fig. 2), it can be seen a diffraction peak appeared at the lower angles of the diffractogram indicated the intercalation of Calix-NH$_2$ molecules in the interlayer spaces of Mt. The ions of the clay mineral were exchanged with ammonium cations of calixarene to prepare the organoclays, and the exchange resulted in an increase in the basal spacing. The basal spacing of Calix-NH$_2$/Mt is increased to 13.06 Å ($2\theta$ = 6.76). The interlayer space height, $\Delta d$, has been calculated as 1.66 Å by subtracting the average layer thickness of Mt (11.4 Å) from that of Calix-NH$_2$/Mt. It is attributed that the cation exchange process achieved between the interlayer cations of Mt and calixarene salt intercalated into the Mt layers.

The thermogravimetric (TG) and derivative thermogravimetric (DTG) curves for pristine Mt and Calix-NH$_2$/Mt are shown in Fig. 3 and 4, respectively. The TGA thermogram of pristine Mt reveals two major temperature regions of mass loss, one below 200 °C and another above 500 °C. The first step observed from room temperature is attributed to the dehydration of physically adsorbed water and dehydration of water molecules adsorbed around metal cations on exchangeable sites in Mt. The last step observed in the temperature region of 500–700 °C is attributed to the dehydroxylation of Mt. After the exchange with the Calix-NH$_2$ salt, thermal decomposition of the Calix-NH$_2$/Mt takes place in three regions. In the first region, below 150 °C, takes place the evolution of adsorbed water. The

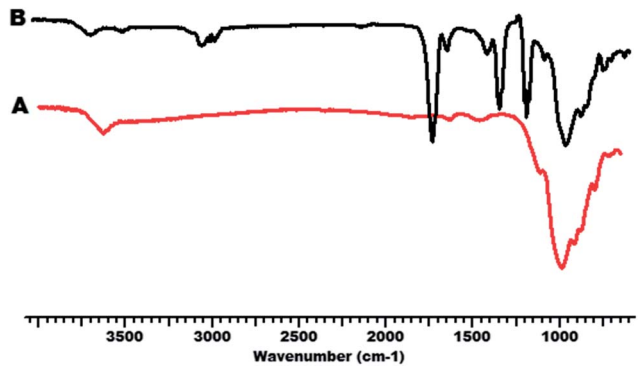


Fig. 1 FTIR spectra of Mt (A) and Calix-NH$_2$/Mt (B).

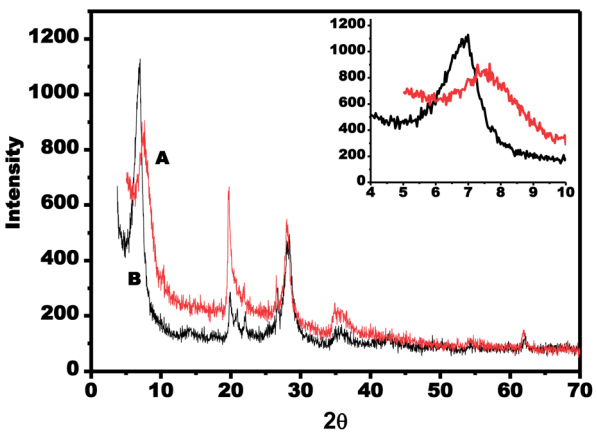


Fig. 2 XRD patterns of Mt (A) and Calix-NH$_2$/Mt (B).

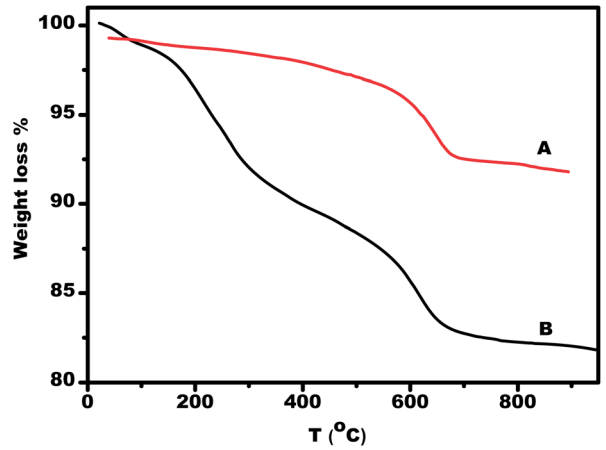


Fig. 3 TG thermograms of Mt (A) and Calix-$NH_2$/Mt (B).

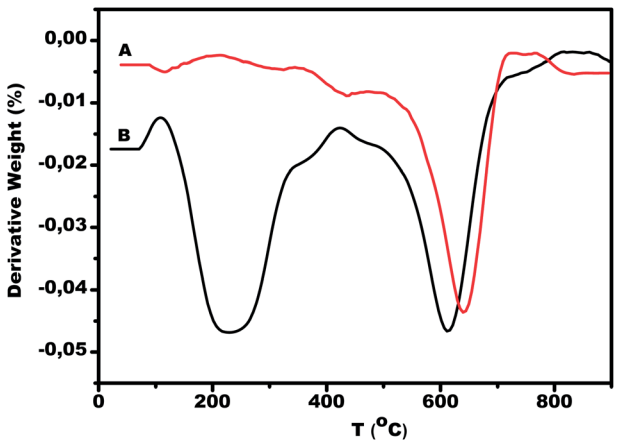


Fig. 4 DTG thermograms of Mt (A) and Calix-$NH_2$/Mt (B).

second region occurs between 400–500 °C due to the decomposition of incorporated organic molecules, and the last one over the temperature range of 600–700 °C which is ascribed to the dehydroxylation of the structural OH units of the organoclay mineral. From Fig. 4, it is observed that the Calix-$NH_2$/Mt presents lower thermal stability than the pristine Mt.

Also, the TGA results were used to examine the amount of organic component. The organic content of the Calix-$NH_2$/Mt was calculated from the residue of the Calix-$NH_2$/Mt after being burnt for over 30 min at 800 °C, using the following equations:[33]

$$\mathrm{Mt}(\%) = \frac{\mathrm{Mt}_{\text{residue at 800 °C}}\%}{0.987} \quad (1)$$

$$\mathrm{Org}\ (\%) = 100\% - \mathrm{Mt}\% \quad (2)$$

The factor of 0.987 in the first equation corrects for loss of physically adsorbed water of the pristine Mt, being in this case 1.3% mass loss as taken from TGA thermogram. From these equations, the amount of organic component is calculated as 16.67%.

The zeta potential is an indicator of the surface charge properties of a colloid or a particle in solution and varies depending on the surface potential and the thickness of the electric double layer. It is usually characterized by the measurement of the electrophoretic mobility of the colloidal particles in dispersion, which is a key technique for the determination of the surface properties of the particles.[34] The zeta potential can be used for studying and predicting colloidal stability and particle surface charge, effectively. It is also an important parameter for a number of applications including characterization of biomedical polymers, electrokinetic transport of particles or blood cells, sensors and biosensors, membrane efficiency and microfluidics.[35–38] In this study, the zeta potentials of the samples were measured as $-42.0 \pm 2.24$ and $-29.70 \pm 0.63$ mV for Mt and Calix-$NH_2$/Mt, respectively. After each modification step, the zeta potentials shifted to less-negative values as a result of adsorption of positively charged calixarene salt at the surface or interlayer of the mineral.

## Optimization studies

Effect of pH and the modifier on the biosensor response were investigated for Calix-$NH_2$/Mt/PyOx biosensor. The effect of pH on the response of the biosensor was studied between pH 5.5 and 7.0 in sodium acetate and sodium phosphate buffer (50 mM) by using glucose (0.25 mM). The lower biosensor response obtained with lower or higher pHs than 6.0. Therefore, pH 6.0 is selected as the optimum for Calix-$NH_2$/Mt/PyOx biosensor (Fig. 5). Previously, the optimum pH was obtained at 10.5 for the PyOx biosensor in which the enzyme was immobilized in the Osmium redox polymer.[25] In another work PyOx immobilized in carbon nanotube modified carbon paste electrode and optimum pH was reported as 7.5.[39] It is known that the optimum pH of free PyOx is 7.0.[40] In our work, optimum working pH of PyOx was shifted to an acidic pH due to the presence of positive groups in the structure of Calix-$NH_2$ intercalated Mt. It is clear that optimum pH is varied depending on the matrices used for the biomolecule immobilization.

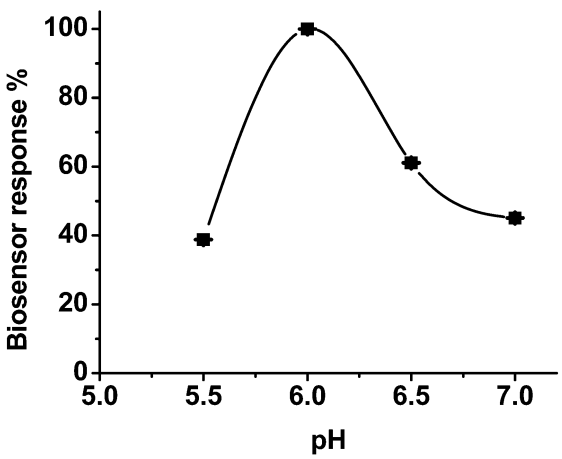


Fig. 5 Effect of pH on the response of Calix-$NH_2$/Mt/PyOx.

Furthermore, the amount of immobilized enzyme affects biosensor sensitivity directly.[41,42] To observe this effect, three different Calix-$NH_2$/Mt biosensors prepared with 0.5 mg, 1.0 and 2.0 mg of PyOx and the amounts of other components were kept constant. Fig. 6 demonstrates that lower enzyme amounts (0.5 mg) cause lower responses due to inadequate enzyme activity. When enzyme amounts were increased to 1.0 mg the highest signal responses were obtained. Furthermore, if 2.0 mg of enzyme was immobilized on the electrode, bioactive layer becomes thicker and this causes decreasing of signals.

Both types of clay mineral samples, pristine and Calix-$NH_2$ modified Mt were applied to examine the effect of Calix-$NH_2$ modification on the biosensor response. The amperometric responses of the Mt/PyOx and Calix-$NH_2$/Mt/PyOx biosensors were linear in the range 0.01–0.5 mM glucose by the equations of $y = 2.33x + 0.03$ ($R^2 = 0.99$) and $y = 3.92x + 0.07$ ($R^2 = 0.99$) respectively. Fig. 7 shows that Calix-$NH_2$/Mt/PyOx biosensor has higher current values as well as higher sensitivity (that can be seen from the slope of the linear graph) in compared to Mt/PyOx.

## Analytical characterization

Calix-$NH_2$/Mt/PyOx biosensor was calibrated under optimum conditions by the addition of glucose standards between 0.01–0.5 mM. All the response signals were measured three times with a 20 s response time. The calibration curve of Calix-$NH_2$/Mt/PyOx biosensor was defined by the equation of $y = 3.16x + 0.02$ ($R^2 = 0.997$) and demonstrated in Fig. 8. Data were given as mean ± S.D. The limit of detection (LOD) was also calculated as 0.50 μM using $S/N = 3$. Various clay mineral based glucose biosensors using laponite,[43,44] alginate/layered double hydroxides,[45] dimethyl and trimethyl modified Mt were reported previously.[17,18] When Calix-$NH_2$/Mt/PyOx is compared with the earlier works, a lower LOD has been observed.[18] The comparison of various PyOx biosensors reported in literature was also given in the ESI as Table S1.†

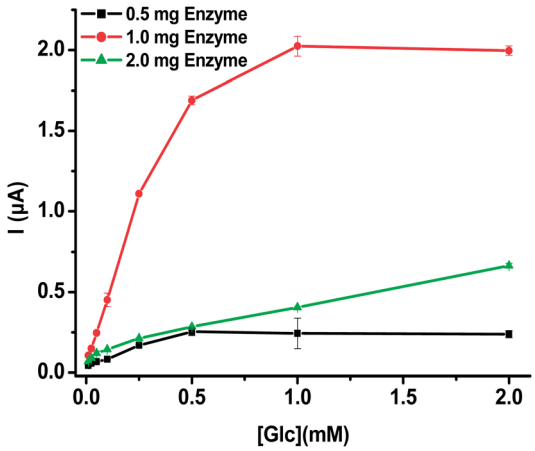


Fig. 6 Effect of enzyme amount on the biosensor response (in sodium phosphate buffer, 50 mM, pH 6.0, at −0.7 V; error bars show standard deviation (S.D) of three measurements).

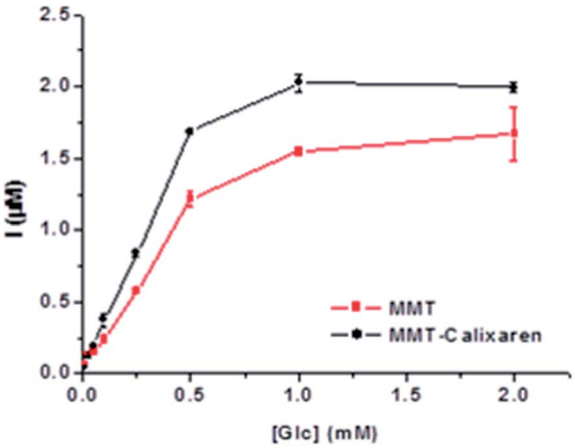


Fig. 7 Effect of the presence of Calix-$NH_2$ as a modifier in the matrix structure on the biosensor response (in sodium phosphate buffer, 50 mM, pH 6.0, at −0.7 V; error bars show S.D of three measurements).

Moreover, repeatability and operational stability of the biosensor were investigated and 10 succeeding measurements were performed using 0.1 mM glucose. The S.D and variation coefficient (c.v) were calculated as 0.1 ± 0.001 mM and 1.06%, respectively. The reproducibility of the biosensor was also evaluated using 4 different enzyme electrodes prepared at different times, using 0.1 mM glucose. The relative standard deviation (RSD) was found as 0.05%. For the operational stability of Calix-$NH_2$/Mt/PyOx biosensor, 80 measurements during 72 h were carried out and after these measurements only 30% decrease was observed. Besides, SEM images, obtained for Mt (Fig. 9A) and Calix-$NH_2$/Mt (Fig. 9B), proved the decoration of Mt with Calix-$NH_2$. The changes in the surface morphologies depending on the modifier types were shown in Fig. 9C and D, respectively. According to these images, it can be said that the

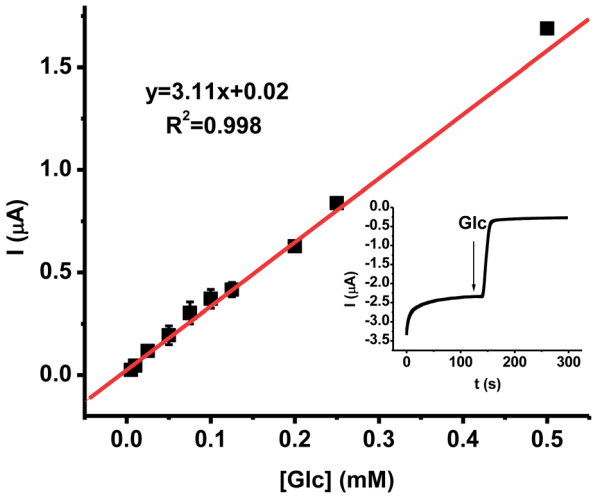


Fig. 8 Calibration curve for glucose (in sodium phosphate buffer, 50 mM, pH 6, −0.7 V; error bars show S.D of three measurements. Inset: time dependent current response with the addition of 0.5 mM glucose).

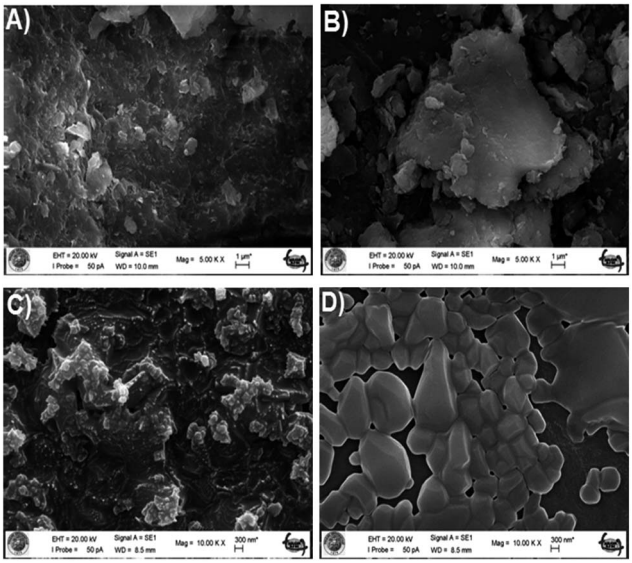


Fig. 9 SEM images of Mt (A), Calix-$NH_2$/Mt (B) with 5000× magnification, Mt/PyOx (C), and Calix-$NH_2$/Mt/PyOx (D) with 10 000× magnification. Scale bars show 1.0 μm for A and B and 300 nm for C and D.

surfaces of Mt/PyOx biosensors were different from Calix-$NH_2$/Mt/PyOx biosensors. In the presence of glutaraldehyde as a cross-linker, covalent bonds between the free amine groups of Calix-$NH_2$, PyOx and BSA were formed and the surface morphology of Calix-$NH_2$/Mt/PyOx biosensors was differentiated from Mt/PyOx biosensors.

### Interferences

Ascorbic acid, uric acid and 3-acetamino phenol (0.1 mM of each compound) were used to evaluate the inference effect on the Calix-$NH_2$/Mt/PyOx biosensor. It is known that at higher potentials, most common metabolites such as uric acid and ascorbic acid get oxidized and interfere with the electrochemical signal.[46] Therefore, effect of interferents to biosensor signals was evaluated by using the working potentials of −0.7 V. The differences in current levels were compared with that of standard glucose solutions and were calculated as a relative response value. Except ascorbic acid, no change was observed in the current response to glucose in the presence of interfering compounds.

### Sample application

Under optimized conditions the glucose concentrations of coke and fizzy were detected using Calix-$NH_2$/Mt/PyOx biosensor. The concentration of glucose in the samples was calculated using the calibration graph. The results were compared with calculated glucose concentrations which were analyzed by reference method (Trinder Reagent) to confirm the accuracy of designed biosensor. The calculated glucose amounts of both samples are shown in Table 1. According to data the use of the Calix-$NH_2$/Mt/PyOx biosensor provided very similar results for the kit data (with the recovery of 99.2%).

Table 1 Glucose content of some beverages obtained by the biosensor and the reference method

| Sample | Calix-$NH_2$/Mt/PyOx (mM ± SD) | Trinder Reactive (mM) | Recovery (%) |
|---|---|---|---|
| Coke | 5.00 ± 0.0 | 5.04 ± 0.1 | 99.2 |
| Fizzy | 5.79 ± 0.47 | 6.0 ± 0.15 | 96.5 |

## Conclusions

In conclusion, a promising material which is a good candidate for several biotechnological applications was synthesized, characterized and applied as an enzyme immobilization and biosensor platform. PyOx was chosen as a model enzyme to fabricate Mt based biosensors. The Calix-$NH_2$/Mt/PyOx sensor has shown good linearity with low detection limit. At the final step, the biosensor was applied for glucose analysis in real samples and the obtained data for the clay biosensor were in good agreement with reference method. This system could apply different bio-analysis systems for the biotechnological applications.

## Acknowledgements

The Authors would like to thank the European Union through the COST Action CM1202 “Supramolecular photocatalytic water splitting (PERSPECT-$H_2O$)” and the Scientific and Technological Research Council of Turkey (TUBITAK Grant Numbers 113T022) for the financial support of this research.

## Notes and references

1 T. R. Oliveira, G. F. Grawe, S. Katiuce Moccelini, A. J. Terezo and M. Castilho, *Analyst*, 2014, **139**, 2214–2220.
2 D. Polcari, A. Kwan, M. R. Van Horn, L. Danis, L. Pollegioni, E. S. Ruthazer and J. Mauzeroll, *Anal. Chem.*, 2014, **86**, 3501–3507.
3 N. C. Bagger, S. F. Badino, R. Tokin, M. Gontsarik, S. Fathalinejad, K. Jensen, M. D. Toscano, T. H. Sorensen, K. Borch, H. Tatsumi, P. Väljamäe and P. Westh, *Enzyme Microb. Technol.*, 2014, **58–59**, 68–74.
4 M. Ammam, *Biosens. Bioelectron.*, 2014, **58**, 121–131.
5 Q. Lang, L. Yin, J. Shi, L. Li, L. Xia and A. Liu, *Biosens. Bioelectron.*, 2014, **51**, 158–163.
6 M. Xia, Y. Jiang, L. Zhao, F. Li, B. Xue, M. Sun, D. Liu and X. Zhang, *Colloids Surf., A*, 2010, **356**, 1–9.
7 Q. Fan, D. Shan, H. Xuea, Y. Hea and S. Cosnier, *Biosens. Bioelectron.*, 2007, **22**, 816–821.
8 J. V. de Melo, S. Cosnier, C. Mousty, C. Martelet and N. Jaffrezic-Renault, *Anal. Chem.*, 2002, **74**, 4037–4043.
9 D. Songurtekin, E. E. Yalcinkaya, D. Ag, M. Seleci, D. Odaci Demirkol and S. Timur, *Appl. Clay Sci.*, 2013, **86**, 64–69.
10 J. M. Zen and C. W. Lo, *Anal. Chem.*, 1996, **68**, 2635–2640.
11 N. Touisni, F. Charmantray, V. Hélaine, L. Hecquet and C. Mousty, *Biosens. Bioelectron.*, 2014, **62**, 90–96.

12 R. I. Iliescu, E. Andronescu, C. D. Ghiţulică, D. Berger and A. Ficai, *Sci. Bull.–Univ. "Politeh." Bucharest, Ser. B*, 2011, **73**, 3–16.
13 B. D. Kevadiya, H. A. Patel, G. V. Joshi, S. H. R. Abdiand and H. C. Baja, *Indian J. Pharm. Sci.*, 2010, **72**, 732–737.
14 D. Kevadiya, G. V. Joshi, H. A. Patel, P. G. Ingole, H. M. Mody and H. C. Bajaj, *J. Biomater. Appl.*, 2010, **25**, 161–176.
15 G. V. Joshi, B. D. Kevadiyaa, H. A. Patel, H. C. Bajaj and R. V. Jasra, *Int. J. Pharm.*, 2009, **374**, 53–57.
16 R. Bongartz, D. Ag, M. Seleci, J. G. Walter, E. E. Yalcinkaya, D. OdaciDemirkol, F. Stahl, S. Timur and T. Scheper, *J. Mater. Chem. B*, 2013, **1**, 522–528.
17 B. Demir, M. Seleci, D. Ag, S. Cevik, E. E. Yalcinkaya, D. Odaci Demirkol, U. Anik and S. Timur, *RSC Adv.*, 2013, **3**, 7513.
18 M. Seleci, D. Ag, E. E. Yalcinkaya, D. Odaci Demirkol, C. Guler and S. Timur, *RSC Adv.*, 2012, **2**, 2112–2118.
19 L. Baldini, A. Casnati, F. Sansone and R. Ungaro, *Chem. Soc. Rev.*, 2007, **36**, 254–266.
20 *Host–Guest Complex Chemistry: Synthesis, Structures, Applications*, ed. F. Voegtle and E. Weber, Springer, Berlin, 1985.
21 R. Ludwig, *Fresenius' J. Anal. Chem.*, 2000, **367**, 103–128.
22 V. Bohmer, *Angew. Chem., Int. Ed. Engl.*, 1995, **34**, 713–745.
23 M. Chen, W. Zhang, R. Jiang and G. Diao, *Anal. Chim. Acta*, 2011, **687**, 177–183.
24 D. Odaci Demirkol, H. B. Yildiz, S. Sayın and M. Yilmaz, *RSC Adv.*, 2014, **4**, 19900–19907.
25 F. Tasca, S. Timur, R. Ludwig, D. Haltrich, J. Volc and R. Antiochia, *Electroanalysis*, 2007, **19**, 294–302.
26 C. D. Gutsche and K. C. Nam, *J. Am. Chem. Soc.*, 1988, **110**, 6153–6162.
27 V. Loon, J. D. Arduini, A. Coppi, L. Verboom, W. Pochini, A. Ungaro, R. Harkema and S. Reinhoudt, *D.N. J. Org. Chem.*, 1990, **55**, 5639–5646.
28 F. Unob, Z. Asfari and J. Vicens, *Tetrahedron Lett.*, 1998, **39**, 2951–2954.
29 B. Balazs, G. Toth, G. Horvath, A. Grün, V. Csokai, L. Töke and I. Bitter, *Eur. J. Org. Chem.*, 2001, 61–71.
30 E. E. Saka and C. Guler, *Clay Miner.*, 2006, **41**, 853–861.
31 P. Trinder, *Ann. Clin. Biochem.*, 1969, **6**, 24–27.
32 F. Bergaya, M. Jaber, J. F. Lambert and M. Galimberti, *Science, Technology and Applications. Hoboken*, Wiley, 2011, pp. 45–86.
33 L. Cui, D. M. Khramovb, C. W. Bielawski, D. L. Hunter, P. J. Yoon and D. R. Paul, *Polymer*, 2008, **49**(17), 3751–3761.
34 E. E. Yalcinkaya and C. Guler, *Sep. Sci. Technol.*, 2010, **45**, 635–642.
35 M. Bauman, A. Kosak, A. Lobnika, I. Petrinic and T. Luxbacher, *Colloids Surf., A*, 2013, **422**, 110–117.
36 J. Yang and D. Y. Kwok, *Anal. Chim. Acta*, 2004, **507**, 39–53.
37 C. Werner, U. Konig, A. Augsburg, C. Arnhold, H. Korber, R. Zimmermann and H.-J. Jacobasch, *Colloids Surf., A*, 1999, **159**, 519–529.
38 C. Mousty, *Anal. Bioanal. Chem.*, 2010, **396**, 315–325.
39 D. OdaciDemirkol, A. Telefoncu and S. Timur, *Sens. Actuators, B*, 2008, **132**, 159–165.
40 I. Nishimura, K. Okada and Y. J. Koyama, *J. Biotechnol.*, 1996, **52**, 11–20.
41 M. Akin, M. Yuksel, C. Geyik, D. Odaci Demirkol, A. Bluma, T. Höpfner, S. Beutel and T. Scheper, *Biotechnol. Prog.*, 2009, **26**, 896–906.
42 M. Yuksel, M. Akin, C. Geyik, D. Odaci Demirkol, C. Ozdemir, A. Bluma, T. Hopfner and S. Beutel, *Biotechnol. Prog.*, 2011, **27**, 530–538.
43 S. Poyard, N. Jaffrezic-Renault, C. Martelet, S. Cosnier, P. Labbe and J. L. Besombes, *Sens. Actuators, B*, 1996, **33**, 44–49.
44 D. Shan, J. Zhang, H. G. Xue, S. N. Ding and S. Cosnier, *Biosens. Bioelectron.*, 2010, **25**, 1427–1433.
45 S. N. Ding, D. Shan, H. G. Xue, D. B. Zhu and S. Cosnier, *Anal. Sci.*, 2009, **25**, 1421–1425.
46 F. Mizutani, Y. Sato, T. Sawaguchi, S. Yabuki and S. Iijima, *Sens. Actuators, B*, 1998, **52**, 23–29.

 